doi:10.1016/j.jmb.2007.04.015 J. Mol. Biol. (2007) 370, 290–302

JMB

Available online at www.sciencedirect.com

ScienceDirect

ELSEVIER

# Solution Structure of the Ubp-M BUZ Domain, a Highly Specific Protein Module that Recognizes the C-terminal Tail of Free Ubiquitin

**Ming-Tao Pai[1], Shiou-Ru Tzeng[2], Jeffrey J. Kovacs[3] Mignon A. Keaton[3], Shawn S.-C. Li[2], Tso-Pang Yao[3] and Pei Zhou[1]***

[1]*Department of Biochemistry Duke University Medical Center, Durham NC 27710, USA*

[2]*Department of Biochemistry and the Siebens-Drake Medical Research Institute, Schulich School of Medicine and Dentistry, University of Western Ontario, London Ontario, Canada N6G 2V4*

[3]*Department of Pharmacology and Cancer Biology, Duke University Medical Center Durham, NC 27710, USA*

**Corresponding author*

The BUZ/Znf-UBP domain is a distinct ubiquitin-binding module found in the cytoplasmic deacetylase HDAC6, the E3 ubiquitin ligase BRAP2/IMP, and a subfamily of deubiquitinating enzymes. Here, we report the solution structure of the BUZ domain of Ubp-M, a ubiquitin-specific protease, and its interaction with ubiquitin. Unlike the BUZ domain from isopeptidase T (isoT) that contains a single zinc finger, the Ubp-M BUZ domain features three zinc-binding sites consisting of 12 residues. These zinc ligands form a pair of cross-braced ring fingers encapsulated within a third zinc finger in the primary structure. In contrast to isoT, which can form an N-terminal loop swapped dimer in the crystal state, the formation of additional zinc fingers in the Ubp-M BUZ domain restricts its N-terminal loop to intra-domain interactions. The ubiquitin-binding site of the Ubp-M BUZ domain is mapped to the highly conserved, concave surface formed by the α3 helix and the central β-sheet. We further show that this site binds to the C-terminal tail of free ubiquitin, and corresponding peptides display essentially the same binding affinities as full-length ubiquitin does for the Ubp-M BUZ domain. However, modification of the $G76_{Ub}$ carboxylate group either by a peptide or isopeptide bond abolishes BUZ–domain interaction. The unique ubiquitin-recognition mode of the BUZ domain family suggests that they may function as "sensors" of free ubiquitin in cells to achieve regulatory roles in many aspects of ubiquitin-dependent processes.



*Keywords:* BUZ domain; Znf-UBP domain; ubiquitin-binding domain; zinc finger

## Introduction

Post-translational modification by ubiquitin plays an important role in many cellular processes, such as transcription, translation, DNA repair, virus budding, protein re-localization, protein degradation by the 26 S proteasome, and cell-cycle progression.[1–7] Ubiquitin is a highly conserved, 76 amino acid residue protein that can be conjugated to target proteins by the concerted actions of a ubiquitin-activating enzyme (E1), a ubiquitin-conjugating enzyme (E2) and a ubiquitin ligase (E3).[3,8] The canonical conjugation reaction occurs between the C-terminal glycine (G76) of ubiquitin and the ε-amino group of a lysine side-chain of the target protein. Additionally, ubiquitin itself can be further conjugated through one of its seven conserved lysine residues, generating poly-ubiquitinated proteins.

Abbreviations used: isoT, isopeptidase T; DUBs, deubiquitinating enzymes; Znf-UBP domain, ubiquitin carboxyl-terminal hydrolase-like zinc finger domain; DAUP domain, deacetylase/ubiquitin-specific protease domain; PAZ domain, polyubiquitin-associated zinc finger domain; BUZ domain, binder of ubiquitin zinc finger domain; USPs, ubiquitin-specific proteases; GST, glutathione-*S*-transferase; NOE, nuclear Overhauser effect; NOESY, NOE spectroscopy; HSQC, heteronuclear single quantum coherence; ITC, isothermal titration calorimetry; ESI, electron spray ionization.

E-mail address of the corresponding author: peizhou@biochem.duke.edu

Similar to protein phosphorylation, the ubiquitination process can be readily reversed *via* actions of deubiquitinating enzymes (DUBs), rendering it a truly flexible signaling tag to regulate many different cellular events.

Various forms of ubiquitination have been implicated in many different pathways.[9,10] For example, K48 poly-ubiquitin linkage targets a substrate protein to degradation by the 26 S proteasome machinery; K63 poly-ubiquitination has been associated with DNA repair; whereas mono-ubiquitination plays important roles in signaling pathways involving membrane protein trafficking, endocytosis, and transcription regulation.[1,4] In order for these different ubiquitin tags to signal in divergent pathways, they must be recognized specifically by distinct ubiquitin-binding domains to transmit proper signals.[11,12] To date, more than 16 distinct motifs have been identified as ubiquitin-binding domains.[13] Although the sizes and topologies of these ubiquitin-binding domains vary, the majority of them interact with the hydrophobic patch centered at I44 of ubiquitin.[14,15] Interestingly, recent biochemical and structural studies revealed several novel ubiquitin-binding domains that associate with ubiquitin without engaging the I44 site. These include the ubiquitin-binding motif (UBM), A20-type zinc finger/Rabex-5 ubiquitin-binding zinc finger (RUZ), and ubiquitin carboxyl-terminal hydrolase-like zinc finger (Znf-UBP) domains.[16–19] Diversity in the binding mode makes it possible for a single ubiquitin molecule to be recognized simultaneously by multiple ubiquitin-binding domains.

The Znf-UBP domain, also known as the DAUP (deacetylase/ubiquitin-specific protease) domain, PAZ (polyubiquitin-associated zinc finger) domain or BUZ (binder of ubiquitin zinc finger) domain, is found in the cytoplasmic deacetylase HDAC6, the E3 ubiquitin ligase BRCA1-associated protein 2 (BRAP2 or impedes mitogenic signal propagation, IMP), and a group of ubiquitin-specific proteases (USPs).[20–24] To emphasize the fact that this domain is distributed beyond ubiquitin-specific proteases, we refer to this domain as the BUZ domain.

The function of the BUZ domain is best characterized in HDAC6. Biochemical analysis *in vitro* demonstrated that the BUZ domain from HDAC6 interacted with mono-ubiquitin as well as with poly-ubiquitin chains. It was further shown that HDAC6 bound to misfolded, ubiquitinated proteins in a BUZ-dependent manner.[25] This latter interaction appears to be important for the turnover of poly-ubiquitinated proteins in cells.[26] Recent biochemical and structural analysis of the isopeptidase T (isoT) BUZ/Znf-UBP domain revealed a distinct ubiquitin-binding mode for this domain characterized by its specific recognition of the C terminus of free ubiquitin, rather than through binding to the canonical hydrophobic surface centered around I44 of ubiquitin.[19] Interestingly, these studies identified a single zinc-binding site in the BUZ/Znf-UBP domain of isoT, whereas biochemical studies of the HDAC6 BUZ domain revealed the existence of three zinc-binding sites,[26] suggesting that the BUZ family can be further divided into different sub-groups depending on the mode of zinc coordination.

Here, we report biochemical and structural characterization of the BUZ domain from Ubp-M (hUSP16) and its interaction with ubiquitin. Ubp-M is a deubiquitinating enzyme in the USP family, and its inactivation blocks progression in the cell cycle.[27] Ubp-M is able to deubiquitinate mono-ubiquitinated nucleosomal histone H2A at the execution phase of apoptosis.[28] Primary structure analysis shows that Ubp-M contains a BUZ domain at its N terminus and a catalytic domain at its C terminus. Mass spectrometric measurements performed on native and denatured Ubp-M BUZ domains identify three zinc ions associated with each folded BUZ molecule, while the solution structure reveals three unique zinc-binding sites arranged in an atypical "cross-braced" ring finger configuration within a third zinc finger.[29,30] We further show that the Ubp-M BUZ domain binds to ubiquitin or corresponding C-terminal peptides with affinities in the low micromolar range. In contrast, the Ubp-M BUZ domain does not recognize peptides with the C-terminal glycine residue blocked either by an extra residue or by a lysine side-chain, suggesting that the BUZ domain recognizes the free C terminus of ubiquitin specifically.

## Results

### Defining the minimal sequence for the BUZ domain in Ubp-M

Because of the functional significance of the HDAC6 BUZ domain in aggresome formation,[25] we initially investigated whether a recombinant BUZ domain fused to glutathione-*S*-transferase (GST) could bind to mono- and/or poly-ubiquitin in an *in vitro* pull-down assay (Figure 1). The wild-type HDAC6 BUZ domain, but not a C1145S or C1145S/H1164A mutant, which alters the conserved and putative zinc-coordinating cysteine and histidine residues, nor GST alone, bound efficiently to both mono-ubiquitin and poly-ubiquitin chains containing a free C terminus; similarly, a related BUZ domain from the human deubiquitinase Ubp-M[27] was capable of binding to mono- and poly-ubiquitin, indicating that ubiquitin-binding is a common property of the BUZ domain family.

Despite repeated attempts, the HDAC6 BUZ domain proved to be a difficult target for NMR analysis (data not shown). We therefore focused our studies on the related BUZ domain from Ubp-M. A construct of Ubp-M containing the N-terminal 134 residues from T10 to S143 encompassing the BUZ domain was over-expressed and purified for preliminary analysis. Triple-resonance NMR experiments were used to assign the backbone resonances of the protein.[31,32] Analysis of the $^{1}H$-$^{15}N$ heteronuclear nuclear Overhauser effect (NOE) spectra

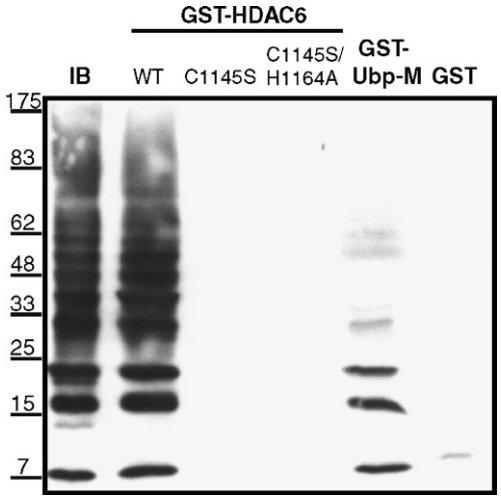


**Figure 1.** The BUZ domain binds to mono- and poly-ubiquitin. Recombinant GST-fusion proteins containing the wild-type BUZ domain from HDAC6 (residues 1044–1273), a C1145S mutation, a C1145S/H1164A mutation, the Ubp-M BUZ domain, or GST alone were incubated with mono-ubiquitin and poly-ubiquitin chains generated *in vitro*. Bound fractions were then subjected to SDS-PAGE analysis and immunoblotted with a ubiquitin antibody (IB).

showed that the N-terminal residues of the Ubp-M BUZ domain, T10 to L20, were disordered (Supplementary Data Figure S1).[33] On the basis of this information, a shorter fragment consisting of P22 to S143 of Ubp-M was cloned and expressed as an N-terminal $His_6$-tagged protein. After $Ni^{2+}$-NTA purification and thrombin cleavage to remove the $His_6$ tag, the remaining fragment, containing an additional GSHM sequence at the N terminus from the expression vector, was renumbered 1–126 for further structural and biochemical studies. Analytical ultracentrifugation analysis of this fragment revealed that the BUZ domain of Ubp-M is monomeric in solution (data not shown).

## The BUZ domain of Ubp-M contains three zinc ions

The existence of a large number of conserved cysteine and histidine residues within the BUZ domain has led to its classification as a zinc-finger-containing domain. We therefore used electron spray ionization (ESI) mass spectrometry to determine the zinc content within the BUZ domain of Ubp-M (Figure 2). The native state of the Ubp-M BUZ domain has a molecular mass of 14,649 Da. When the protein was denatured in 50% (v/v) acetonitrile containing 0.1% (v/v) trifluoroacetic acid, its molecular mass decreased to 14,459 Da, in agreement with the theoretical value of 14,459.3 Da. The difference of 190 Da in molecular mass between the native and denatured Ubp-M BUZ domains corresponds to a loss of three zinc ions. Although for proper protein folding the bacterial growth medium contained 100 μM $ZnSO_4$, no zinc was supplied during the extensive purification process that should have removed any non-specifically bound zinc ions. On the basis of the

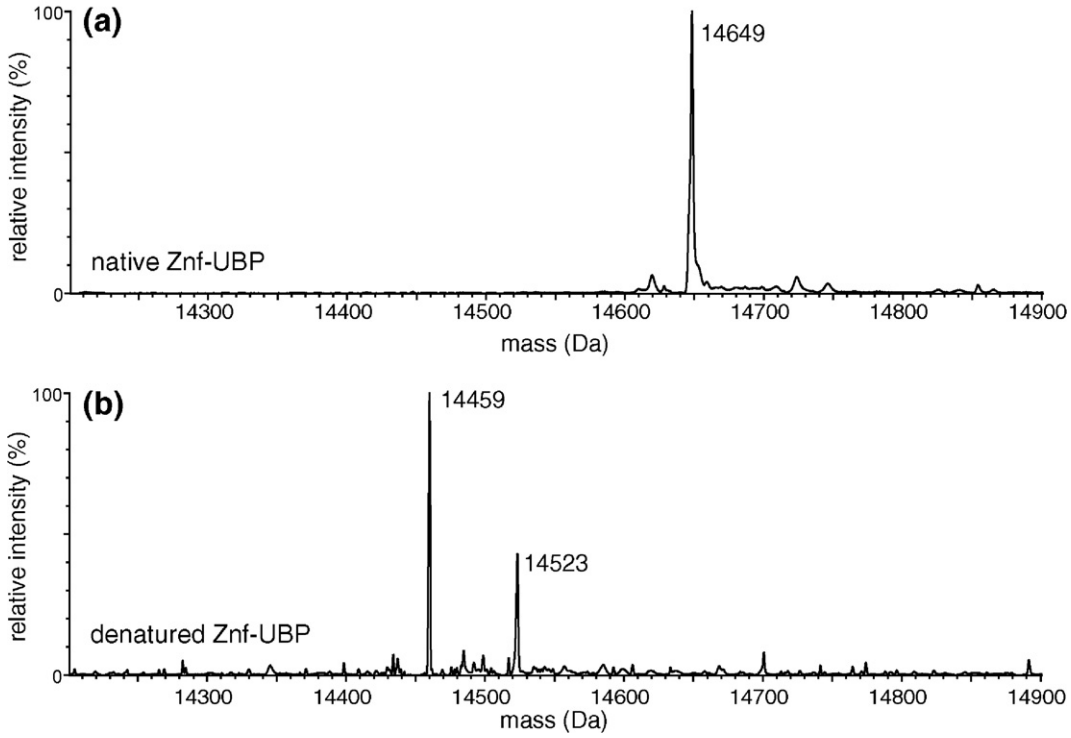


**Figure 2.** Mass spectrometric analysis reveals three zinc ions in the Ubp-M BUZ domain. The difference in molecular mass between the (a) native and (b) denatured proteins corresponds to the loss of three zinc ions.

mass spectrometric analysis, we concluded that the BUZ domain of Ubp-M contains three zinc-binding sites.

In addition to the main peak of 14,459 Da, a smaller peak of molecular mass 14,523 Da appeared in the spectrum of the denatured protein

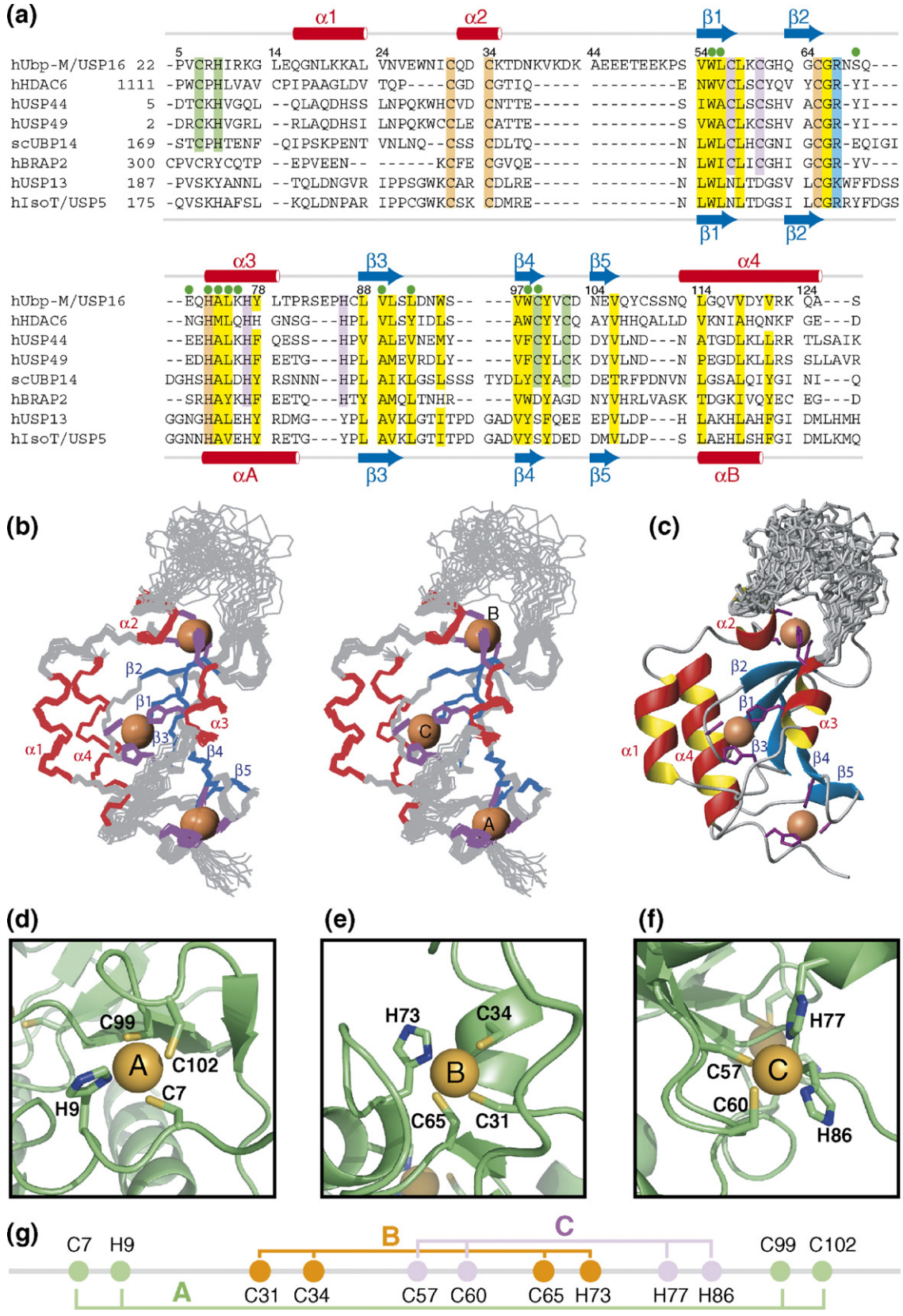


**Figure 3** (*legend on next page*)

(Figure 2(b)). The molecular mass of this peak corresponds to that of the Ubp-M BUZ domain containing one zinc ion, suggesting that the affinity of one particular zinc-binding site in the Ubp-M BUZ domain is significantly greater than the remaining two.

Although our studies establish three zinc ions in the Ubp-M BUZ domain, the number of zinc-binding sites appears to vary among different members of the BUZ family. For example, the recent crystal structure of the isoT BUZ/Znf-UBP domain revealed a single zinc-binding site,[19] whereas particle-induced X-ray emission studies suggested the existence of three zinc ions in the HDAC6 BUZ domain.[26] Our observation of three zinc ions in the Ubp-M BUZ domain highlights its similarity to the HDAC6 BUZ domain. This assessment is further supported by the conservation of 12 potential zinc-chelating residues in the primary structures among the BUZ domains of Ubp-M, HDAC6 and a number of other ubiquitin-specific proteases (Figure 3(a)). However, the majority of these zinc ligands are not conserved in the BUZ domain of isoT, suggesting that Ubp-M and isoT employ different architectures for zinc coordination.

## Solution structure of the BUZ domain of Ubp-M

The structure of the BUZ domain of Ubp-M was determined by NMR on the basis of 3458 NOE, 144 dihedral angle, and 60 hydrogen bond restraints, and was further refined with 102 residual dipolar couplings. Excluding the disordered residues at the N and C termini (1–6 and 126) and the internally disordered loop (residues 36–53), the mean pairwise rmsd values of backbone and heavy atoms of the NMR ensemble (Figure 3(b)) are 0.49 Å and 0.85 Å, respectively. Additional statistics are shown in Table 1.

The solution structure (Figure 3(b) and (c)) of the Ubp-M BUZ domain contains four α-helices and five β-strands held together by three distinct zinc-binding sites. The β-strands are arranged in an antiparallel fashion to form a twisted β-sheet located at the center. This central β-sheet is sandwiched on one side by helices α1 and α4 oriented in parallel with each other, and on the other side by helix α3. The edge of the β-sheet (β2) is flanked by a short α2 helix, with the C terminus of α2 separated from the central β-sheet by a 14 residue disordered insert loop found only in Ubp-M.

**Table 1.** Structural statistics for the Ubp-M BUZ domain (20 structures)

| | |
|---|---|
| NOE distance restraints | 3458 |
| Intra-residue | 1578 |
| Sequential ($\|i–j\| = 1$) | 673 |
| Medium-range ($2 \le \|i–j\| \le 4$) | 530 |
| Long-range ($\|i–j\| \ge 5$) | 677 |
| Hydrogen bonds[a] | 60 |
| Dihedral angle constraints | 144 |
| Residual dipolar couplings ($^1D_{NH}$) | 51 |
| Residual dipolar couplings ($^1D_{CH}$) | 51 |
| Dipolar coupling *R* factor of $^1D_{NH}$[b] (%) | 14.3±0.2 |
| Dipolar coupling *R* factor of $^1D_{CH}$[c] (%) | 15.9±0.6 |
| Ramachandran plot[c] | |
| Favored regions (%) | 92.0 |
| Allowed regions (%) | 98.4 |
| *Deviations from idealized geometry* | |
| Bond lengths (Å) | 0.015±0.000 |
| Bond angles (deg.) | 1.724±0.031 |
| Improper angles (deg.) | 1.799±0.083 |
| *Mean pairwise rmsd* | |
| Backbone (residues 7–35, 54–125) (Å) | 0.49 |
| Heavy atoms (residues 7–35, 54–125) (Å) | 0.85 |

None of these structures exhibit distance violations greater than 0.5 Å or dihedral angle violations greater than 5°.

[a] Two constraints per hydrogen bond ($d_{HN\text{-}O} \le 2.0$ Å and $d_{N\text{-}O} \le 3.0$ Å) are implemented for amide protons protected from solvent-exchange.

[b] *R*-factor for residual dipolar coupling is defined as the ratio of the r.m.s deviation between observed and calculated values to the expected r.m.s deviation if the vectors were distributed randomly.[52]

[c] MOLPROBITY was used to assess the quality of the structures.[49,50]

The Ubp-M BUZ domain features three well-defined zinc-binding sites formed by eight cysteine and four histidine residues. Each zinc-binding site contains four residues with their respective side-chains positioned ideally for tetrahedral zinc coordination (Figure 3(d)–(f)).

The first zinc-binding site consists of residues C7, H9, C99 and C102 (finger A, Figure 3(d)). The formation of this $C_3H$-type zinc finger positions the N terminus of the BUZ domain to the vicinity of the loop connecting β4 and β5 of the central β-sheet. The second zinc-binding site, also belonging to the $C_3H$ type, is formed by two cysteine residues (C31 and C34) in the CXXC motif of α2, C65 at the C terminus of β2, and H73 at the N terminus of α3 (finger B, Figure 3(e)). The last zinc-binding site

**Figure 3.** Solution structure of the Ubp-M BUZ domain. (a) Sequence alignment of representative BUZ domains from hUbp-M (NP_006438), hHDAC6 (NP_006035), hUSP44 (AAH30704), hUSP49 (NP_061031), scUBP14 (NP_009614), hBRAP2 (NP_006759), hUSP13 (NP_003931), and hIsoT (NP_003472). Conserved residues are highlighted, with hydrophobic and glycine residues colored yellow, basic residues blue, and residues involved in zinc binding pale green, brown, and purple, according to the formation of individual zinc fingers. The majority of these conserved residues are located in the central β-sheet and α3, which comprise the ubiquitin-binding interface. Secondary structures are labeled. Residues that experience chemical shift perturbation upon ubiquitin binding are denoted by green dots above the sequence. The NMR ensemble and the ribbon diagram of the Ubp-M BUZ domain are shown in (b) and (c), respectively. Secondary structures are highlighted, with helices in red and strands in blue. The zinc ions (brown) are shown in a sphere. Details of the three zinc-binding sites are shown in (d)–(f), with side-chains of zinc ligands shown as sticks. The topology of the three zinc fingers in the primary structure is shown in (g).

belongs to the $C_2H_2$ type, and consists of two cysteine residues in the second CXXC motif (C57 at the C terminus of β1 and C60 in the β1-β2 loop), H77 at the C terminus of α3, and H86 in the loop connecting α3 and β3 (finger C, Figure 3(f)). Residues of the second and third zinc-binding sites do not form typical zinc fingers, but adopt a cross-braced ring finger structure instead.[29,30] These ring fingers position α2 to the edge and α3 on top of the central β-sheet to generate a concave surface encircled by α3 and the twisted β-sheet for ubiquitin recognition. Interestingly, these ring finger residues are located entirely between the residues of the first zinc-binding site in the primary structure, featuring an atypical topology of zinc coordination uniquely found in the BUZ domain of Ubp-M.

## The BUZ Domain of Ubp-M binds to the free C-terminal tail of Ubiquitin

We investigated the binding interface between the Ubp-M BUZ domain and ubiquitin by NMR titration experiments. To map the BUZ-binding site on ubiquitin, a series of $^{1}H$-$^{15}N$ heteronuclear single quantum coherence (HSQC) spectra of $^{15}N$-labeled human ubiquitin were recorded in the presence of increasing molar ratios of the unlabeled Ubp-M BUZ domain. Surprisingly, ubiquitin residues forming the hydrophobic patch centered at I44, a common binding site for most known ubiquitin-binding domains, did not experience any noticeable perturbation in chemical shifts. On the contrary, the backbone resonances of L73, R74, G75 and G76, and side-chain resonances of Q41 were broadened severely during titration. Moreover, the amide resonances of V70 and R72 were perturbed progressively by the Ubp-M BUZ domain in a concentration-dependent manner. The majority of these perturbed residues map exclusively to the C-terminal tail of ubiquitin (Figure 4(a) and (d)).

In order to determine the ubiquitin-binding site on the BUZ domain, a reciprocal titration was performed by adding incremental amounts of unlabeled ubiquitin to an $^{15}N$-labeled Ubp-M BUZ domain sample. A number of resonances were perturbed in the resulting $^{1}H$-$^{15}N$ HSQC spectra (Figure 4 and Supplementary Data Figure S2). The side-chain resonance of W55 and backbone resonances of L56, S69, E71, H73, A74, L75, K76, V89, L92, W98, and C99 of the Ubp-M BUZ domain were either perturbed severely or exchange-broadened during titration. These residues are located in a pocket encircled by helix α3 and strands β1, β3, and β4 of the central β-sheet (Figures 3(a) and 4). In contrast, addition of C-terminal $His_6$-tagged ubiquitin to the $^{15}N$-labeled BUZ domain sample did not result in any noticeable chemical shift perturbation, suggesting that the BUZ domain of Ubp-M does not recognize ubiquitin with its C-terminal glycine residue (G76) blocked. This mode of ubiquitin binding by the Ubp-M BUZ domain is reminiscent of the recognition of the ubiquitin C terminus by the isoT BUZ/Znf-UBP domain.[19]

## The Ubp-M BUZ domain binds to ubiquitin and ubiquitin C-terminal peptides with similar affinities

The C-terminal tail of ubiquitin, consisting of residues L73–G76, forms a disordered loop that extends beyond the globular fold of ubiquitin. Because our NMR titration data suggest that the BUZ domain of Ubp-M interacts with the C terminus of ubiquitin, we examined whether the BUZ domain could bind to the corresponding peptide with high affinity. A peptide, *YA*-RLRGG, was therefore synthesized that contained the last five residues of ubiquitin (residues 72–76) and two additional residues, *YA*, at the N terminus to facilitate concentration measurement by UV absorbance. The peptide–BUZ domain interaction was first evaluated by NMR titration. Interestingly, this peptide induced an HSQC chemical shift perturbation pattern in the Ubp-M BUZ domain identical with that of the full-length ubiquitin (Figure 4(c)), suggesting that the interaction between ubiquitin and the Ubp-M BUZ domain is mediated predominantly by the C-terminal peptide of ubiquitin.

To evaluate this unique interaction between the Ubp-M BUZ domain and the ubiquitin C-terminal peptide in more quantitative terms, we measured the corresponding dissociation constant by isothermal titration calorimetry (ITC) and/or by fluorescence polarization (Figure 5). As a control, we also determined the dissociation constant of the Ubp-M BUZ-ubiquitin complex by ITC and obtained a $K_d$ of 6.53 μM. This value is similar to that of the isoT BUZ/Znf-UBP–ubiquitin complex. Importantly, the Ubp-M BUZ domain bound to the ubiquitin peptide *YA*-RLRGG with a $K_d$ of 15.88 μM. Extending this peptide by three residues toward the N terminus to include residues L69, V70, and L71 of ubiquitin further enhanced the binding affinity of the resulting peptide (*YA*-LVLRLRGG). The resulting $K_d$ of 6.77 μM is essentially identical with that of ubiquitin for the Ubp-M BUZ domain (Table 2). These data suggest that residues important for interacting with the Ubp-M BUZ domain reside exclusively in the C-terminal tail of ubiquitin, and that the BUZ domain is a protein-recognition as well as a peptide-recognition module.

## The BUZ domain does not recognize C-terminally modified ubiquitin peptides

We next examined whether the Ubp-M BUZ domain could recognize the same peptides containing either an extra residue at the C terminus (f-*YA*-RLRGGD, where f denotes a fluorescein moiety, see Table 2) or an isopeptide bond formed between the carboxyl group of the G76 and the ε-amino group of a lysine side-chain (f-*YA*-RLRGG-isoK or f-*YA*-LVLRLRGG-isoK, Table 2). The latter modification is frequently encountered in poly-ubiquitinated proteins. These C-terminally modified peptides, unlike the ubiquitin peptides containing free C termini, completely lost the ability to interact with

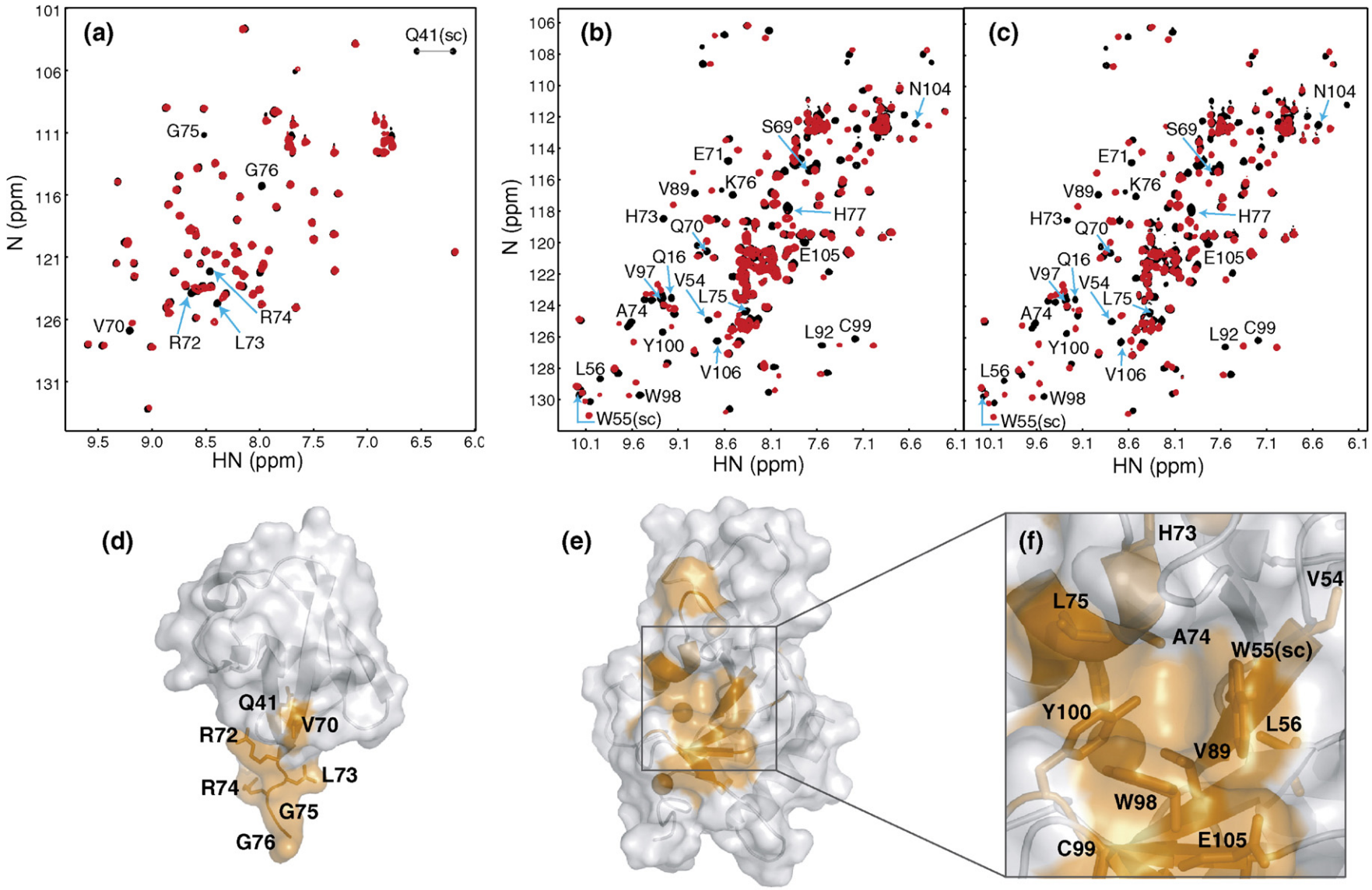


**Figure 4.** NMR titration maps the binding interface to the concaved surface of the BUZ domain of Ubp-M and the C-terminal tail of ubiquitin. (a) $^{1}H$-$^{15}N$ HSQC spectra of ubiquitin in the absence (black) and in the presence (red) of the Ubp-M BUZ domain. $^{1}H$-$^{15}N$ spectra of Ubp-M in the absence (black) and in the presence (red) of ubiquitin or the ubiquitin peptide *YA*-RLRGG are shown in (b) and (c), respectively. (d) A surface representation of ubiquitin with significantly perturbed residues labeled in black and colored orange. (e) and (f) Surface representations of the Ubp-M BUZ domain with significantly perturbed residues labeled in black and colored orange.

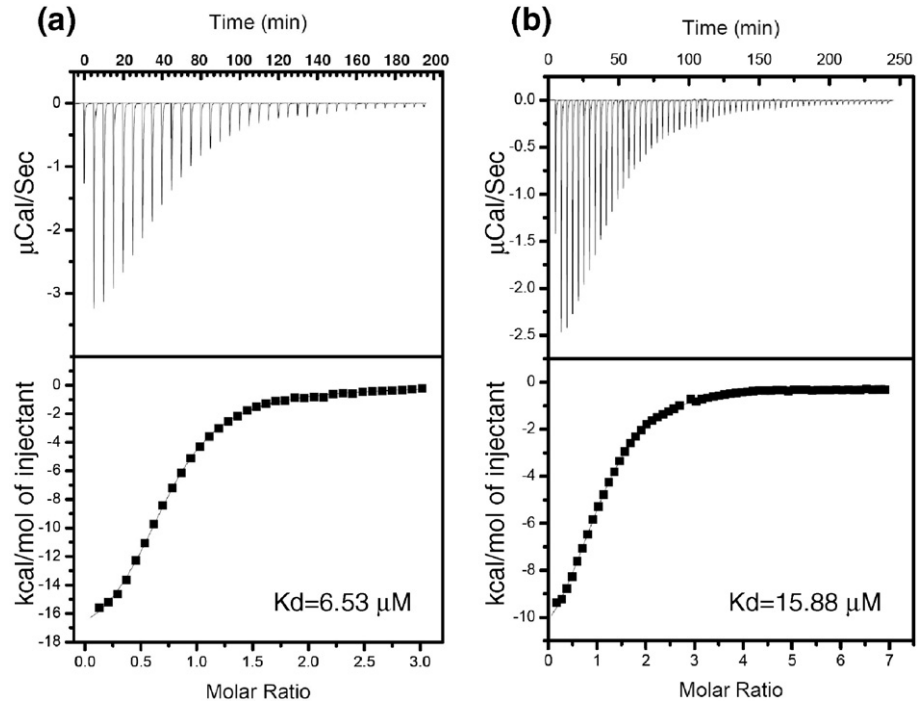


**Figure 5.** The BUZ domain of Ubp-M binds to ubiquitin and a ubiquitin C-terminal peptide *YA*-RLRGG with similar affinities. ITC analyses of the BUZ domain interactions with ubiquitin and the ubiquitin peptide *YA*-RLRGG are shown in (a) and (b), respectively.

the Ubp-M BUZ domain (Table 2). These observations suggest that the BUZ domain of Ubp-M does not recognize a peptide bond connecting linear ubiquitin modules nor an iso-peptide bond found in poly-ubiquitinated proteins.

## Discussion

### Structural comparison between the BUZ domains of Ubp-M and IsoT

The overall fold of the BUZ/Znf-UBP domains of Ubp-M and isoT is similar and features a central, twisted β-sheet with two prominent helices packed on both sides of the β-sheet (helices α3 and α4 in Ubp-M, and αA and αB in isoT) (Figure 6). In particular, residues located on the secondary structure elements (α3, β1, β3, and β4) that make up the ubiquitin-binding pocket are highly conserved (Figure 3(a)). Consistent with this observation, the backbone traces of α3 and the central β-sheet of the Ubp-M BUZ domain are essentially superimposable upon those of isoT, with a backbone rmsd of ~0.5 Å (Figure 6, boxed regions).

There are, however, significant differences between these two domains (Figure 6). First, in the crystal structure of the isoT BUZ/Znf-UBP domain, residues N-terminal to β1 form an extended loop devoid of any regular secondary structures that crosses the edge of the entire β-sheet. The formation of a $C_3H$-type zinc finger in the isoT BUZ/Znf-UBP domain restricts the C-terminal end of this loop to the tip of β2 and αA, whereas the N-terminal portion of the loop engages the tip of β4 and β5 of the central β-sheet *via* electrostatic interactions mediated by residues R174, K178, H179, D257 and D262. This N-terminal portion of the loop appears to be flexible and contributes to the dimer interface in the crystal structures either through a disulfide-bonded bridge or as a domain-swapped loop. In contrast, the corresponding residues in the BUZ domain of Ubp-M assume a more rigid conformation and are engaged exclusively in intra-domain interactions. The very N-terminal part of the loop is restrained to the tip of β4 and β5 by a zinc finger (finger A). Immediately following this zinc finger, there are two helices, α1 and α2. The α1 helix is oriented in parallel with the α4 helix to cross the top of β1 and β2, and the α2 helix is held to strand β2 and helix α3 by a second zinc finger (finger B). In comparison, no regular secondary structure is ob-

**Table 2.** Binding affinities of the Ubp-M BUZ domain for ubiquitin or ubiquitin-derived peptides

| Name | Sequences | $K_d$ (μM) | Method |
|---|---|---|---|
| Ubiquitin | WT ubiquitin | 6.5 | ITC |
| Pentapeptide | *YA*-RLRGG-COOH | 15.9 | ITC |
| f-pentapeptide | f-*YA*-RLRGG-COOH | 15.9 | FP |
| f-octapeptide | f-*YA*-LVLRLRGG-COOH | 6.8 | FP |
| f-penta-D | f-*YA*-RLRGGD | TLQ | FP |
| f-penta-isoK | f-*YA*-RLRGG-isoK | TLQ | FP |
| f-octa-isoK | f-*YA*-LVLRLRGG-isoK | TLQ | FP |

*YA*, residues added to aid determination of the concentration; f, fluorescein; TLQ,: affinity too low for accurate quantification; ITC, isothermal titration calorimetry; FP, fluorescence polarization.

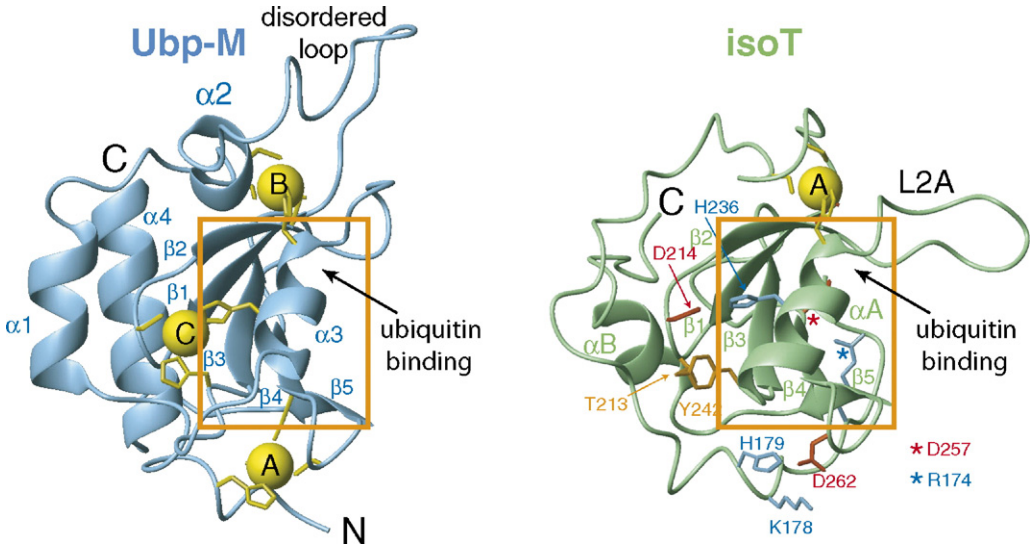


**Figure 6.** Structural comparison of the BUZ domains of Ubp-M and isoT. Ribbon diagrams of Ubp-M and isoT are colored pale blue and pale green, respectively. Secondary structures and zinc fingers are denoted. Boxed regions indicate the highly conserved BUZ domain interface for ubiquitin binding, which consists of a central β-sheet and an α-helix (α3 in Ubp-M or αA in isoT). Residues of isoT that replace the structural role of the two structural zinc fingers A and C of Ubp-M are shown as sticks and are labeled, with hydrophobic residues colored brown, basic residues blue, and acidic residues red.

served in the isoT BUZ/Znf-UBP domain in the regions corresponding to helices α1 and α2 of the Ubp-M BUZ domain.

Second, despite a high degree of sequence conservation of α3 residues involved in ubiquitin binding, the packing of α3 against the central β-sheet is supported by distinct mechanisms in Ubp-M when compared with isoT, in which the corresponding helix (αA) interacts with the β-sheet through a salt-bridge between residues D214 and H236 and van der Waals contacts between residues T213 and Y242; whereas in Ubp-M, such interactions are functionally replaced by yet another zinc finger (finger C) that mediates the packing of α3 against the β-sheet (Figure 6).

Third, the C-terminal helix (α4) in Ubp-M is significantly longer and is oriented differently from the corresponding helix (αB) of isoT. In Ubp-M, α4 packs parallel to α1 across the back of the central β-sheet, whereas the corresponding helix (αB) in isoT interacts with the N-terminal extended loop and is buttressed by an insert loop connecting strands β3 and β4 (Figure 6).

Finally, the BUZ/Znf-UBP domain of isoT contains an insertion loop (L2A) between β2 and αA, which was proposed to form a "ruler loop" to interact with ubiquitin.[19] Interestingly, such a loop is absent from Ubp-M. Instead, Ubp-M contains a unique insert loop between α2 and β1. Compared with the ruler loop in isoT, the insert loop in Ubp-M is longer (14 amino acid residues). Surprisingly, this loop is completely disordered and its resonances are not affected by ubiquitin binding, suggesting that this insert loop is unlikely to be involved in ubiquitin binding.

## Zinc fingers contribute to the structural integrity of the BUZ domain

Our mass spectrometry and NMR studies of the BUZ domain of Ubp-M unambiguously established three zinc ions in the native protein that are coordinated by 12 residues in the form of cross-braced ring fingers encapsulated within another zinc finger in the primary structure. These zinc ligands are conserved in HDAC6, but not in isoT, suggesting that the zinc-binding modes of the BUZ domains of HDAC6 and Ubp-M are identical, but they differ from that of isoT. The existence of multiple zinc fingers in the BUZ domains of Ubp-M and HDAC6 are crucial for maintaining their structural integrity. Mutation of any of the zinc-binding residues in the BUZ domain of HDAC6 resulted in a loss of ubiquitin interaction, presumably due to impaired folding.[26] Similarly, point mutations of zinc-binding residues (C31S, C57S, H77S, H86S, or C99S) in the BUZ domain of Ubp-M led to protein degradation manifested by the production of proteolytic fragments during protein expression (data not shown).

Based on this current study and the difference in zinc-binding configurations, we propose to further classify the BUZ domain family into three subgroups. The BUZ domains of Ubp-M, HDAC6, hUSP44, hUSP49, and scUSP14 form the first group since each contains 12 conserved zinc-coordinating residues and is expected to bind three zinc ions using two $C_3H$ and one $C_2H_2$ fingers. In contrast, the BUZ domain of either isoT or hUSP13 contains a single $C_3H$ zinc finger, and thus belongs to a different sub-group. The functions of the two other zinc fingers found in the first group are replaced

here by hydrophobic and electrostatic interactions. The hBRAP2 BUZ domain differs from the above two groups in that it harbors nine out of 12 residues involved in the formation of zinc-binding sites in the first group. Because these residues span only two of the three zinc fingers, we propose that the hBRAP2 BUZ domain belongs to a third group and likely contains cross-braced ring-fingers of the $C_3H$ and $C_2H_2$ types.

### Biological implications

The finding that the BUZ domain from Ubp-M binds free glycine at the C terminus of ubiquitin indicates that this domain should not be able to bind ubiquitin or ubiquitin chains that are conjugated to protein substrates. Such a binding mode would be consistent with the idea that this domain anchors free poly-ubiquitin chains for further processing by deubiquitinating enzymes, such as Ubp-M or isoT. This assertion, however, is not entirely consistent with the observation that HDAC6 can bind poly-ubiquitinated proteins (Figure 7(a)) and the BUZ domain is crucial for such interactions.[25] These apparent contradictory findings might be resolved if the BUZ domain in HDAC6 does not bind directly to poly-ubiquitinated proteins, but rather serves to modulate the binding activity of HDAC6. Supporting this view, unlike HDAC6, Ubp-M does not bind poly-ubiquitinated proteins appreciably in response to proteasome inhibition (Figure 7(a)). We speculate that by virtue of its unusually high affinity for the free ubiquitin, the BUZ domain would normally be occupied by free ubiquitin or poly-ubiquitin chains, and this interaction inhibits HDAC6 binding to poly-ubiquitinated proteins. When the cellular ubiquitin pool is reduced, a condition often associated with decreased proteasome activity and the accumulation of misfolded proteins, the BUZ domain would be emptied, and the resulting conformational switch could allow HDAC6 for binding to poly-ubiquitinated proteins (Figure 7(b)), and transporting ubiquitinated proteins to aggresomes and autophagy.[25] Although it remains possible that the BUZ domain takes part in the binding of ubiquitinated proteins by a yet to be defined mechanism, our studies suggest that the BUZ domain, at the minimum, would be required for activating the poly-ubiquitinated protein-binding activity of HDAC6 by "sensing" the levels of cellular ubiquitin pool. Such a model would suggest that the BUZ domain operates as a regulatory domain that modulates protein deacetylase, E3 ligase and deubiquitinating enzyme function in response to changes in local or cellular levels of free ubiquitin and/or poly-ubiquitin chains. If such a model is correct, proteins with the BUZ domain would act commonly as sensors for cellular ubiquitin status and likely play important roles in many aspects of ubiquitin-dependent processes.

## Materials and Methods

### Ubiquitin binding assay

GST or GST-fusion proteins were purified using glutathione-Sepharose resin (GE Healthcare, Piscataway, NJ). Protein levels were normalized by measuring the absorbance at 595 nm ($A_{595}$). Purified protein on beads was then incubated with 1 μg of *in vitro* synthesized mono- and poly-ubiquitin chains (Affiniti Bioreagents, Golden, CO) in NETN buffer,[34] containing 1 mM BSA to prevent the re-absorption of ubiquitin, at 4 °C for 3 h. Samples were subjected to SDS-PAGE, and then immunoblotted for ubiquitin.

For ubiquitinated protein binding *in vivo*, 293T cells were transfected with empty vector, pCDNA3-Flag-HDAC6,[25] or pCDNA3-Flag-UbpM constructs. These transfected cells were treated with 5 μM MG132 (Sigma-Aldrich, St. Louis, MO) for 12–16 h, and then lysed in NETN buffer in the presence of 5 mM *N*-ethylmaleimide (NEM, Sigma-Aldrich). Flag-tagged proteins were immunoprecipitated

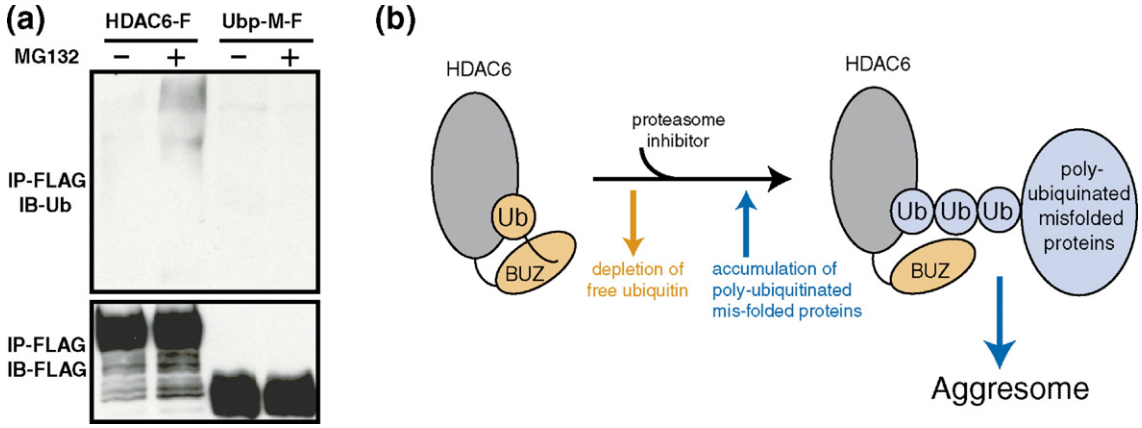


**Figure 7.** Proteasome inhibitors induce specific association of poly-ubiquitinated proteins with HDAC6, but not with Ubp-M. (a) FLAG-HDAC6 or FLAG-UbpM expression plasmids were transfected into 394T cells and treated with MG132 as indicated. HDAC6 and UbpM were immuno-precipitated by anti-FLAG (M2) antibody followed by immuno-blotting with a ubiquitin antibody. (b) A potential model for the association of HDAC6 with poly-ubiquitinated proteins. In this model, depletion of free ubiquitin enables binding of HDAC6 to poly-ubiquitinated proteins.

from 500 μg of lysate with anti-Flag antibody and protein G Sepharose. Binding of ubiquitinated proteins was determined by immunoblotting with anti-ubiquitin and anti-Flag antibodies.

### Sample preparation

The BUZ domain constructs of Ubp-M encoding residues T10 to S143, or P22 to S143 were cloned into a pET15b vector (EMD Biosciences, Inc., Madison, WI) between NdeI and BamHI sites, and were over-expressed as N-terminal $His_6$-tagged proteins in *Escherichia coli* BL21(DE3)STAR cells (Invitrogen Inc., Carlsbad, CA). Bacterial cells were initially grown in Luria broth or M9 minimal medium at 37 °C. After the $A_{600}$ reached 0.6, the cells were induced with 0.2 mM isopropyl-β-D- thiogalactopyranoside (IPTG) and 100 μM $ZnSO_4$ at 20 °C for 15 h before harvest. Isotopically labeled proteins were overexpressed in M9 medium supplemented with [$^{15}$N]$NH_4Cl$ and [$^{13}$C]glucose as the sole nitrogen and carbon sources. NMR samples were prepared with uniform $^{15}$N, $^{13}$C,$^{15}$N, or 10% $^{13}$C labeling.

The N-terminal $His_6$-tagged fusion constructs containing T10-S143 or P22-S143 of Ubp-M were purified by passage through a $Ni^{2+}$-NTA column and treated with thrombin to remove the $His_6$ tags. The resulting fragments, containing an additional four residues (GSHM) at the N terminus and residues 10–143 or 22–143 of Ubp-M, were further purified by size-exclusion chromatography. All NMR samples were exchanged into a buffer containing 25 mM sodium phosphate, 100 mM KCl, 2 mM DTT, and 5% or 100% $^2H_2O$ (pH 7.0) before experiments. Samples were degassed and sealed under argon to prevent cysteine oxidation.

Human ubiquitin with a cleavable N-terminal $His_6$ tag was cloned into the pET15b vector, expressed and purified essentially as described for the BUZ domain of Ubp-M except that bacterial cells were induced with 1 mM IPTG at 37 °C for 4 h. A second ubiquitin construct containing a non-cleavable C-terminal $His_6$ tag was prepared as a negative control.

### ESI mass spectrometry

ESI mass spectrometry was performed on the native and denatured proteins using a quadrupole time-of-flight mass spectrometer (Q-TOF 2) (Waters Corporation, Milford, MA) run in the positive ion electrospray mode. A stock solution of the Ubp-M BUZ domain was diluted into 25 mM $NH_4HCO_3$ to maintain the native state, whereas the denatured state was obtained by dissolving the protein sample in a solution containing 50% (v/v) acetonitrile and 0.1% (w/v) formic acid. Data were processed using the MaxEnt1 algorithm provided in MassLynx4.0 to yield the average mass for native and denatured proteins.

### NMR structure determination

All NMR experiments were performed at 27 °C using Varian INOVA 600 or 800 MHz spectrometers. Data were processed by NMRPIPE and analyzed with XEASY/CARA.[35,36] Backbone resonances were collected by standard 3D triple-resonance experiments and analyzed using PACES;[37] side-chain resonances were assigned using 3D HCCH-TOCSY and 2D homonuclear TOCSY and NOESY experiments.[31,32] Distance constraints were derived from three-dimensional $^{15}$N and $^{13}$C-separated NOESY-HSQC experiments.[31] Dihedral angles were derived from the combined input of TALOS analysis based on chemical-shift information, $^3J_{HNH\alpha}$ couplings determined from an HNHA experiment, and analysis of local NOE patterns.[38–40] Stereo-specific assignments of valine and leucine methyl groups were obtained *via* a high-resolution $^1$H-$^{13}$C HSQC spectrum of a 10% $^{13}$C-labeled sample.[41] Initial structures were generated with CYANA.[42,43] Because both the $N^{\delta1}$ and $N^{\varepsilon2}$ atoms of histidine residues can potentially be involved in zinc binding, we evaluated the zinc-coordination geometry of these histidine residues individually, assuming either $N^{\delta1}$ or $N^{\varepsilon2}$ as the zinc ligand. Only one combination (H9 $N^{\delta1}$, H73 $N^{\delta1}$, H77 $N^{\varepsilon2}$, and H86 $N^{\delta1}$) satisfied all experimental constraints, and was used to calculate the final ensemble of NMR structures. Three zinc ions were included during the final stages of structure calculations.

Residual dipolar couplings ($^1D_{HN}$ and $^1D_{H\alpha C\alpha}$) were determined from the difference of couplings between an isotropic medium and a liquid crystalline Pf1 phage medium (~12 mg/ml) in 25 mM sodium phosphate, 400 mM potassium chloride, 15% $^2H_2O$ (pH 7.0). The 3D HNCO-based experiments were used to measure the $^1D_{HN}$ and $^1D_{H\alpha C\alpha}$ couplings.[44,45] These residual dipolar couplings were used for structure refinement using XPLOR-NIH with a water-refinement protocol.[46–48] Out of 40 calculated structures, 20 were selected for presentation based on the optimal geometry evaluated by MOLPROBITY.[49,50] The statistics of the NMR ensemble are shown in Table 1.

### Peptide synthesis

Peptides corresponding to the C-terminal tail of ubiquitin or lysine-conjugated ubiquitin were synthesized using standard Fmoc (*N*-(9-fluorenyl)methoxycarbonyl) chemistry on a 431A peptide synthesizer (Applied Biosystems, Foster City, CA). For peptides used for fluorescence polarization measurements, an appropriate amount of 5-(and-6)-carboxy-fluorescein succinimidyl ester was added to the peptide resin, and the coupling reaction was allowed to proceed for 1 h at room temperature. The peptides were cleaved from the resin by treatment with trifluoroacetic acid and purified by reverse-phase HPLC using a C18 column.[51] The sequences of the peptides are listed in Table 2. The identity of the peptides was confirmed by mass spectrometry.

### NMR titration studies

The binding site of ubiquitin was mapped by recording a series of $^1$H-$^{15}$N HSQC spectra of $^{15}$N-labeled ubiquitin with increasing molar ratios (from 1:0 to 1:2) of the unlabeled Ubp-M BUZ domain. Similarly, a series of $^1$H-$^{15}$N HSQC spectra were recorded for the $^{15}$N labeled Ubp-M BUZ domain in the presence of increasing molar ratios (from 1:0 to 1:2) of unlabeled ubiquitin or synthetic peptides to map the binding surface of the BUZ domain. Chemical-shift perturbations were calculated as:

$$\delta_{CS} = \sqrt{(\delta_{HN})^2 + (0.2\delta_N)^2}$$

using resonances of $^{15}$N Ubp-M or $^{15}$N ubiquitin in the presence of 2:1 molar ratios of unlabeled ubiquitin or Ubp-M, respectively.

### Isothermal titration calorimetry

The Ubp-M BUZ domain, ubiquitin, and a peptide (*YA*-RLRGG) containing the last five residues of ubiquitin were exchanged into a buffer containing 25 mM sodium phosphate and 100 mM KCl at pH 7.0. ITC measurements were performed on a MicroCal VP-ITC instrument (MicroCal, LLC, Northampton, MA). Raw data were obtained from 30 automatic injections of 10 μl aliquots of 1.5 mM ubiquitin into a solution of 50 μM Ubp-M BUZ domain at 20 °C. Data were fit using Origin 7.0 (OriginLab Corporation, Northampton, MA) according to a 1:1 binding model.

### Fluorescence polarization measurements

Fluorescence polarization experiments were conducted at 20 °C on a Beacon 2000 Polarization System (PanVera, Madison, WI). An incremental amount of the purified Ubp-M BUZ domain was titrated into a fluorescent peptide solution containing 20 mM sodium phosphate, 100 mM NaCl, pH 7.0, and the resulting polarization values were recorded. Binding data were fit to a hyperbolic nonlinear regression model using Prism 3.0 (GraphPad Software, Inc., San Diego, CA).

### Protein Data Bank accession code

Atomic coordinates have been deposited with the RCSB Protein Data Bank (PDB entry 2I50).

## Acknowledgements

We thank Martha G. Bomar, Qian Liu, and Cheng-Yu Chen for assistance with cloning and protein purification, and Lu Han for synthesizing the peptides used in this work. This work was supported by the Whitehead Foundation (to P.Z.), a Canadian Institute of Health Research (CIHR) grant (to S.S.C.L.), and a National Institute of Health grant (NS054022 to T.P.Y.).

## Supplementary Data

Supplementary data associated with this article can be found, in the online version, at doi:10.1016/j.jmb.2007.04.015

## References

1. Welchman, R. L., Gordon, C. & Mayer, R. J. (2005). Ubiquitin and ubiquitin-like proteins as multifunctional signals. *Nature Rev. Mol. Cell Biol.* **6**, 599–609.
2. Muratani, M. & Tansey, W. P. (2003). How the ubiquitin-proteasome system controls transcription. *Nature Rev. Mol. Cell Biol.* **4**, 192–201.
3. Hershko, A. & Ciechanover, A. (1998). The ubiquitin system. *Rev. Biochem. Annu.* **67**, 425–479.
4. Hicke, L. (2001). Protein regulation by monoubiquitin. *Nature Rev. Mol. Cell Biol.* **2**, 195–201.
5. Sun, L. & Chen, Z. J. (2004). The novel functions of ubiquitination in signaling. *Curr. Opin. Cell Biol.* **16**, 119–126.
6. Conaway, R. C., Brower, C. S. & Conaway, J. W. (2002). Emerging roles of ubiquitin in transcription regulation. *Science*, **296**, 1254–1258.
7. Huang, T. T. & D'Andrea, A. D. (2006). Regulation of DNA repair by ubiquitylation. *Nature Rev. Mol. Cell Biol.* **7**, 323–334.
8. Pickart, C. M. (2001). Mechanisms underlying ubiquitination. *Ann. Rev. Biochem.* **70**, 503–533.
9. Weissman, A. M. (2001). Themes and variations on ubiquitylation. *Nature Rev. Mol. Cell Biol.* **2**, 169–178.
10. Pickart, C. M. & Fushman, D. (2004). Polyubiquitin chains: polymeric protein signals. *Curr. Opin. Chem. Biol.* **8**, 610–616.
11. Buchberger, A. (2002). From UBA to UBX: new words in the ubiquitin vocabulary. *Trends Cell Biol.* **12**, 216–221.
12. Hicke, L., Schubert, H. L. & Hill, C. P. (2005). Ubiquitin-binding domains. *Nature Rev. Mol. Cell Biol.* **6**, 610–621.
13. Hurley, J. H., Lee, S. & Prag, G. (2006). Ubiquitin-binding domains. *Biochem. J.* **399**, 361–372.
14. Beal, R. E., Toscano-Cantaffa, D., Young, P., Rechsteiner, M. & Pickart, C. M. (1998). The hydrophobic effect contributes to polyubiquitin chain recognition. *Biochemistry*, **37**, 2925–2934.
15. Mueller, T. D. & Feigon, J. (2002). Solution structures of UBA domains reveal a conserved hydrophobic surface for protein-protein interactions. *J. Mol. Biol.* **319**, 1243–1255.
16. Penengo, L., Mapelli, M., Murachelli, A. G., Confalonieri, S., Magri, L., Musacchio, A. *et al.* (2006). Crystal structure of the ubiquitin binding domains of Rabex-5 reveals two modes of interaction with ubiquitin. *Cell*, **124**, 1183–1195.
17. Lee, S., Tsai, Y. C., Mattera, R., Smith, W. J., Kostelansky, M. S., Weissman, A. M. *et al.* (2006). Structural basis for ubiquitin recognition and autoubiquitination by Rabex-5. *Nature Struct. Mol. Biol.* **13**, 264–271.
18. Bienko, M., Green, C. M., Crosetto, N., Rudolf, F., Zapart, G., Coull, B. *et al.* (2005). Ubiquitin-binding domains in Y-family polymerases regulate translesion synthesis. *Science*, **310**, 1821–1824.
19. Reyes-Turcu, F. E., Horton, J. R., Mullally, J. E., Heroux, A., Cheng, X. & Wilkinson, K. D. (2006). The ubiquitin binding domain ZnF UBP recognizes the C-terminal diglycine motif of unanchored ubiquitin. *Cell*, **124**, 1197–1208.
20. Hook, S. S., Orian, A., Cowley, S. M. & Eisenman, R. N. (2002). Histone deacetylase 6 binds polyubiquitin through its zinc finger (PAZ domain) and copurifies with deubiquitinating enzymes. *Proc. Natl Acad. Sci. USA*, **99**, 13425–13430.
21. Seigneurin-Berny, D., Verdel, A., Curtet, S., Lemercier, C., Garin, J., Rousseaux, S. & Khochbin, S. (2001). Identification of components of the murine histone deacetylase 6 complex: link between acetylation and ubiquitination signaling pathways. *Mol. Cell Biol.* **21**, 8035–8044.
22. Kovacs, J. J., Hubbert, C. & Yao, T. P. (2004). The HDAC complex and cytoskeleton. *Novartis Found Symp.* **259**, 170–181.
23. Asada, M., Ohmi, K., Delia, D., Enosawa, S., Suzuki, S., Yuo, A. *et al.* (2004). Brap2 functions as a cytoplasmic retention protein for p21 during monocyte differentiation. *Mol. Cell Biol.* **24**, 8236–8243.

24. Matheny, S. A., Chen, C., Kortum, R. L., Razidlo, G. L., Lewis, R. E. & White, M. A. (2004). Ras regulates assembly of mitogenic signalling complexes through the effector protein IMP. *Nature*, **427**, 256–260.
25. Kawaguchi, Y., Kovacs, J. J., McLaurin, A., Vance, J. M., Ito, A. & Yao, T.-P. (2003). The deacetylase HDAC6 regulates aggresome formation and cell viability in response to misfolded protein stress. *Cell*, **115**, 727–738.
26. Boyault, C., Gilquin, B., Zhang, Y., Rybin, V., Garman, E., Meyer-Klaucke, W. *et al.* (2006). HDAC6-p97/VCP controlled polyubiquitin chain turnover. *EMBO J.* **25**, 3357–3366.
27. Cai, S. Y., Babbitt, R. W. & Marchesi, V. T. (1999). A mutant deubiquitinating enzyme (Ubp-M) associates with mitotic chromosomes and blocks cell division. *Proc. Natl Acad. Sci. USA*, **96**, 2828–2833.
28. Mimnaugh, E. G., Kayastha, G., McGovern, N. B., Hwang, S. G., Marcu, M. G., Trepel, J. *et al.* (2001). Caspase-dependent deubiquitination of monoubiquitinated nucleosomal histone H2A induced by diverse apoptogenic stimuli. *Cell Death Differ.* **8**, 1182–1196.
29. Borden, K. L. & Freemont, P. S. (1996). The RING finger domain: a recent example of a sequence-structure family. *Curr. Opin. Struct. Biol.* **6**, 395–401.
30. Saurin, A. J., Borden, K. L., Boddy, M. N. & Freemont, P. S. (1996). Does this have a familiar RING? *Trends Biochem. Sci.* **21**, 208–214.
31. Clore, G. M. & Gronenborn, A. M. (1993). *NMR of Proteins.* CRC Press, Boca Raton, FL.
32. Ferentz, A. E. & Wagner, G. (2000). NMR spectroscopy: a multifaceted approach to macromolecular structure. *Quart. Rev. Biophys.* **33**, 29–65.
33. Kay, L. E., Torchia, D. A. & Bax, A. (1989). Backbone dynamics of proteins as studied by 15N inverse detected heteronuclear NMR spectroscopy: application to staphylococcal nuclease. *Biochemistry*, **28**, 8972–8979.
34. Hubbert, C., Guardiola, A., Shao, R., Kawaguchi, Y., Ito, A., Nixon, A. *et al.* (2002). HDAC6 is a microtubule-associated deacetylase. *Nature*, **417**, 455–458.
35. Delaglio, F., Grzesiek, S., Vuister, G. W., Zhu, G., Pfeifer, J. & Bax, A. (1995). NMRPipe: a multidimensional spectral processing system based on UNIX pipes. *J. Biomol. NMR*, **6**, 277–293.
36. Bartels, C., Xia, T., Billeter, M., Güntert, P. & Wüthrich, K. (1995). The program XEASY for computer-supported NMR spectral analysis of biological macromolecules. *J. Biol. NMR*, **6**, 1–10.
37. Coggins, B. E. & Zhou, P. (2003). PACES: Protein sequential assignment by computer-assisted exhaustive search. *J Biomol. NMR*, **26**, 93–111.
38. Cornilescu, G., Delaglio, F. & Bax, A. (1999). Protein backbone angle restraints from searching a database for chemical shift and sequence homology. *J Biomol. NMR*, **13**, 289–302.
39. Wang, A. C. & Bax, A. (1996). Determination of the backbone dihedral angles f in human ubiquitin from reparameterized empirical Karplus equations. *J. Am. Chem. Soc.* **118**, 2483–2494.
40. Vuister, G. W. & Bax, A. (1993). Quantitative *J* correlation: a new approach for measuring homonuclear three-bond J(HNHa) coupling constants in $^{15}$N-enriched proteins. *J. Am. Chem. Soc.* **115**, 7772–7777.
41. Szyperski, T., Neri, D., Leiting, B., Otting, G. & Wüthrich, K. (1992). Support of $^{1}$H NMR assignments in proteins by biosynthetically directed fractional $^{13}$C-labeling. *J. Biomol. NMR*, **2**, 323–334.
42. Herrmann, T., Güntert, P. & Wüthrich, K. (2002). Protein NMR structure determination with automated NOE assignment using the new software CANDID and the torsion angle dynamics algorithm DYANA. *J. Mol. Biol.* **319**, 209–227.
43. Güntert, P. (2004). Automated NMR structure calculation with CYANA. *Methods Mol. Biol.* **278**, 353–378.
44. Yang, D., Venters, R. A., Mueller, G. A., Choy, W. Y. & Kay, L. E. (1999). TROSY-based HNCO pulse sequences for the measurement of $^{1}$HN-$^{15}$N, $^{15}$N-$^{13}$CO, $^{1}$HN-$^{13}$CO, $^{13}$CO-$^{13}C^{\alpha}$ and $^{1}$HN-$^{13}C^{\alpha}$ dipolar couplings in $^{15}$N, $^{13}$C, $^{2}$H-labeled proteins. *J. Biomol. NMR*, **14**, 333–343.
45. Yang, D., Tolman, J. R., Goto, N. & Kay, L. E. (1998). An HNCO-based pulse scheme for the measurement of $^{13}C^{\alpha}$-$^{1}H^{\alpha}$ one-bond dipolar couplings in $^{15}$N, $^{13}$C labeled proteons. *J. Biomol. NMR*, **12**, 325–332.
46. Schwieters, C. D., Kuszewski, J. J., Tjandra, N. & Clore, G. M. (2003). The Xplor-NIH NMR molecular structure determination package. *J. Magn. Reson.* **160**, 65–73.
47. Linge, J. P., Williams, M. A., Spronk, C. A., Bonvin, A. M. & Nilges, M. (2003). Refinement of protein structures in explicit solvent. *Proteins:Struct. Funct. Genet.* **50**, 496–506.
48. Nabuurs, S. B., Nederveen, A. J., Vranken, W., Doreleijers, J. F., Bonvin, A. M., Vuister, G. W. *et al.* (2004). DRESS: a database of REfined solution NMR structures. *Proteins:Struct. Funct. Genet.* **55**, 483–486.
49. Davis, I. W., Murray, L. W., Richardson, J. S. & Richardson, D. C. (2004). MOLPROBITY: structure validation and all-atom contact analysis for nucleic acids and their complexes. *Nucl. Acids Res.* **32**, W615–W619.
50. Lovell, S. C., Davis, I. W., Arendall, W. B., 3rd, de Bakker, P. I., Word, J. M., Prisant, M. G. *et al.* (2003). Structure validation by Cα geometry: ϕ,ψ and $C^{\beta}$ deviation. *Proteins:Struct. Funct. Genet.* **50**, 437–450.
51. Jia, C. Y., Nie, J., Wu, C., Li, C. & Li, S. S. (2005). Novel Src homology 3 domain-binding motifs identified from proteomic screen of a Pro-rich region. *Mol. Cell Proteomics*, **4**, 1155–1166.
52. Clore, G. M. & Garrett, D. S. (1999). *R*-factor, free *R*, and complete cross-validation for dipolar coupling refinement of NMR structures. *J. Am. Chem. Soc.* **121**, 9008–9012.


***Edited by P. Wright***

*(Received 12 February 2007; received in revised form 30 March 2007; accepted 3 April 2007)*
Available online 12 April 2007